

Selective permeability barrier to urea in shark rectal gland

Joshua D. Zeidel,*^{1,2} John C. Mathai,*^{1,2} John D. Campbell,² Wily G. Ruiz,¹
Gerard L. Apodaca,¹ John Riordan,^{2,3} and Mark L. Zeidel^{1,2}

¹Laboratory of Epithelial Cell Biology, Renal-Electrolyte Division and Department of Medicine, University of Pittsburgh School of Medicine, Pittsburgh, Pennsylvania; ²Mount Desert Island Biological Laboratories, Bar Harbor, Maine; and ³Mayo Clinic Foundation, Scottsdale, Arizona

Submitted 16 December 2004; accepted in final form 22 January 2005

Zeidel, Joshua D., John C. Mathai, John D. Campbell, Wily G. Ruiz, Gerard L. Apodaca, John Riordan, and Mark L. Zeidel. Selective permeability barrier to urea in shark rectal gland. *Am J Physiol Renal Physiol* 289: F83–F89, 2005. First published February 22, 2005; doi:10.1152/ajprenal.00456.2004.—Elasmobranchs such as the dogfish shark *Squalus acanthius* achieve osmotic homeostasis by maintaining urea concentrations in the 300- to 400-mM range, thus offsetting to some degree ambient marine osmolalities of 900–1,000 mosmol/kgH₂O. These creatures also maintain salt balance without losing urea by secreting a NaCl-rich (500 mM) and urea-poor (18 mM) fluid from the rectal gland that is isotonic with the plasma. The composition of the rectal gland fluid suggests that its epithelial cells are permeable to water and not to urea. Because previous work showed that lipid bilayers that permit water flux do not block flux of urea, we reasoned that the plasma membranes of rectal gland epithelial cells must either have aquaporin water channels or must have some selective barrier to urea flux. We therefore isolated apical and basolateral membranes from shark rectal glands and determined their permeabilities to water and urea. Apical membrane fractions were markedly enriched for Na-K-2Cl cotransporter, whereas basolateral membrane fractions were enriched for Na-K-ATPase. Basolateral membrane osmotic water permeability (P_f) averaged $4.3 \pm 1.3 \times 10^{-3}$ cm/s, whereas urea permeability averaged $4.2 \pm 0.8 \times 10^{-7}$ cm/s. The activation energy for water flow averaged 16.4 kcal/mol. Apical membrane P_f averaged $7.5 \pm 1.6 \times 10^{-4}$ cm/s, and urea permeability averaged $2.2 \pm 0.4 \times 10^{-7}$ cm/s, with an average activation energy for water flow of 18.6 kcal/mol. The relatively low water permeabilities and high activation energies argue strongly against water flux via aquaporins. Comparison of membrane water and urea permeabilities with those of artificial liposomes and other isolated biological membranes indicates that the basolateral membrane urea permeability is fivefold lower than would be anticipated for its water permeability. These results indicate that the rectal gland maintains a selective barrier to urea in its basolateral membranes.

elasmobranchs; apical and basal membrane permeability; membrane vesicles

ELASMOBRANCHS AND TELEOSTS maintain plasma and tissue electrolyte compositions and osmolalities distinct from those of the surrounding ocean, which has an osmolality of 1,000 mosmol/kgH₂O (1, 8, 10). Marine teleosts maintain a serum osmolality of 330 mosmol/kgH₂O by drinking and absorbing the NaCl and free water in seawater and selectively excreting the NaCl across the gills, thereby retaining the water (14). By contrast, elasmobranchs, such as *Squalus acanthius* (dogfish), maintain

a serum osmolality at or just above that of seawater by keeping plasma and tissue urea concentrations at 300 mM (1, 8, 10, 14).

Elasmobranchs achieve volume homeostasis, in part, by excreting excess salt and water through the rectal gland (4). Because this tissue provides an excellent model of chloride-secreting epithelia, it has been extensively studied. Depending on the volume status of the animal, a 1-kg dogfish excretes 0.5–2.2 ml/h of rectal gland fluid. The elaborated fluid is isotonic with the plasma but has a higher NaCl concentration (500 mM in the rectal gland fluid compared with 340–350 mM in plasma) and a strikingly low urea concentration (18 mM in the rectal gland fluid compared with 330 mM in plasma) (2, 3).

In prior studies examining water and urea permeabilities of liposomes of varying lipid composition, we reported that water and urea permeabilities vary linearly among liposomes of different composition so that if a given lipid exhibited a low water permeability, it would also exhibit a low urea permeability (10, 18). Because the rectal gland secretes a fluid isotonic with its plasma, one would anticipate that water permeability of the rectal gland epithelium should be high. However, as the gland maintains a striking gradient for urea, the urea permeability should be low. Considering the data from liposomes, rapid water permeation and a permeability barrier to urea could be achieved by the presence of aquaporin water channels or by a selective permeability barrier to urea in the apical or basolateral membranes of rectal gland epithelial cells. To determine whether the rectal gland has functioning aquaporins or a selective barrier to urea, we prepared vesicles highly purified for apical or basolateral plasma membranes and determined the permeabilities of these fractions to water and urea. The results provide strong evidence for a selective barrier to urea flux in the apical and basolateral membranes of the rectal gland epithelium.

MATERIALS AND METHODS

Preparation of apical and basolateral membranes from shark rectal gland. Dogfish were obtained by local fisherman from Frenchman's Bay (Mount Desert Island, ME) and environs. Fifteen to seventeen dogfish were killed by pithing, and their rectal glands were rapidly removed and placed on ice. The preparative protocol of Dubinsky and Monti (6) was followed with minor modifications. Briefly, freshly obtained glands were minced into fragments of ~1 mm³ on an ice-cooled glass surface using dual scalpels and homogenized in ~5 vol of 25 mM HEPES, pH 7.6, containing 1 mM EDTA, 50 mM mannitol, and 10 mM 5,6 carboxyfluorescein (CF). Subsequent steps used buffer containing no CF. Following successive centrifugations at 3,000 and 13,000 g for 15 min each, microsomal

* J. D. Zeidel and J. C. Mathai contributed equally to this study.

Address for reprint requests and other correspondence: M. L. Zeidel, Dept. of Medicine, Univ. of Pittsburgh School of Medicine, Rm. 1218 Scaife Hall, 3500 Terrace St., Pittsburgh, PA 15215 (E-mail: Zeidel@MSX.Dept-med.pitt.edu).

The costs of publication of this article were defrayed in part by the payment of page charges. The article must therefore be hereby marked "advertisement" in accordance with 18 U.S.C. Section 1734 solely to indicate this fact.

membranes were pelleted from the second supernatant at 33,000 *g* for 90 min. An aliquot of these membranes was set aside for purity determinations. The pellet was resuspended in 5 mM HEPES, pH 7.6, and 100 mM mannitol and layered on a linear 5–25% sucrose gradient formed in 20 mM HEPES, pH 7.6, and 1 M KBr. Gradients were centrifuged at 137,000 *g* in a swinging bucket rotor for 2 h with slow acceleration and without brake. The upper apical and lower basolateral bands in the positions noted by Dubinski and Monti (6) were removed by needle aspiration, resuspended, and diluted in the same solution in which the sample had been applied to the gradient, pelleted, and finally resuspended in 10 mM HEPES, pH 7.6, 250 mM sucrose (R buffer). The resulting fractions were collected and washed two to three times with R buffer to remove extravesicular fluorescein [28,000 rpm (141,000 *g*) in SW 28 rotor for 30 min]. The final pellets were resuspended in small volumes of buffer for measurement of markers of purity and permeability measurements. SDS-PAGE in 6% acrylamide gels was performed as we described elsewhere (17) and Western blots were probed with mouse monoclonal antibody 60.1 raised against the COOH-terminal 20 amino acids of shark cystic fibrosis transmembrane regulator (CFTR) and with a commercially available antibody against Na-K-ATPase.

Permeability measurements. Permeabilities to water and urea were measured at 15°C or below (unless otherwise stated) by stopped-flow fluorometry as previously described in detail (5, 16, 18). This lower temperature was used because we observed that vesicle preparations from teleosts and elasmobranchs taken from Maine waters become unstable at temperatures higher than 20°C (10). Briefly, permeabilities were determined using a stopped-flow fluorometer (SX.17 MV, Applied Photophysics, Leatherhead, UK) with a measurement dead-time of <1 ms. To determine osmotic water permeability (P_f), vesicles containing 10 mM CF were rapidly mixed with an equal volume of R buffer (apical membranes) or sucrose buffer (basolateral membranes) that had three times the osmolality due to sucrose addition. Buffer osmolalities were determined using a Wescor vapor pressure osmometer. The rate of water efflux from vesicles was measured as a function of vesicle shrinkage and CF self-quenching. Typically, 8–10 quench curves were averaged and fit with a single exponential curve. Durations of measurements were adjusted to ensure that the entire time course of vesicle shrinkage was examined. To ensure that the only signal recorded was from intravesicular fluorescence, quenching anti-CF antibody (Molecular Probes) was added before the experiment. From parameters that included the initial rate of fluorescence change, vesicle diameter, and applied osmotic gradient, P_f was calculated using MathCad software (MathSoft, Cambridge, MA) as described earlier (10, 11, 16, 18). Urea permeabilities were assayed by incubating membrane vesicles in R buffer containing 1 M urea for 30 min on ice. Rapid mixing of urea-loaded vesicles 1:1 with R buffer containing 0.82 M sucrose (isoosmotic with respect to urea-containing buffer) permitted measurement of urea permeability rates. Urea efflux in response to the chemical gradient is followed by water efflux with subsequent vesicle shrinkage. Flux curves are representative of similar results on three to four membrane preparations. Urea permeability coefficients were determined as described (9, 16, 18) and data are reported as means \pm SE. Measurements of water flux were performed on three separate preparations at varying temperatures to obtain activation energies; three measurements were performed for water permeability at 8.8°C. As it happened, the only temperature that was exactly the same for all three water flux measurements was 8.8°C. For urea permeability, measurements were made for all three preparations at 15.0°C. We chose this temperature because it was well below the level where the preparations began to deteriorate and at the higher end of our range of study to permit optimal loading of urea into the vesicles before the efflux measurements.

Activation energy coefficient calculation. Water permeabilities were measured at five different temperatures between 4 and 18°C. Activation energy (E_a) was calculated from the slope of the natural log of the rate plotted against $1/T$, multiplied by the gas constant, R .

Determination of vesicle size. Vesicle size distribution was determined by quasi-elastic light scattering using a DynaPro LSR particle sizer (Charlottesville, VA) and DYNAMICS data collection and analysis software. Representative size distribution tracings for apical and basolateral membrane vesicles are shown in Fig. 1. Apical membrane vesicles averaged 126 nm in radius, whereas basolateral membrane vesicles averaged 188 nm.

Determination of rectal gland apical and basolateral membrane surface areas. The rectal gland consists of thousands of individual secretory tubules. To our knowledge, there have been no published measurements of the surface areas of apical and basolateral membranes of these tubules. This information is required if we are to compare our measured permeability values to the known rates of water and urea excretion by the rectal glands in sharks. To determine these surface areas, rectal glands were sectioned in coronal and transverse planes and standard stereological analysis was performed. Briefly, shark rectal glands were perfusion fixed using 4% (wt/vol) paraformaldehyde and 0.1% (vol/vol) glutaraldehyde in shark rectal gland buffer (300 mM HEPES, 3% sucrose) and then placed overnight in 60% (wt/vol) sucrose in water. Each gland was rinsed with phosphate-buffered saline and then cut perpendicular to the long axis of the gland into serial 5-mm tissue blocks. The first cut was uniform random in the first 5-mm interval. The tissue blocks were transferred to 30% (wt/vol) sucrose dissolved in phosphate-buffered saline. The blocks were then randomly rotated and then placed in flat molds with the cut surface facing upwards. The orientation of the tissue block was noted, and then the blocks were frozen in Optimal Tissue Cutting (OCT; Sakura Finetech USA, Torrance, CA) reagent by placing the molds on dry ice blocks. Each tissue block was sectioned in a Leica CM 1900 Cryotome (4- μ m thickness) and vertical tissue sections that included the whole block face were adhered to Superfrost slides (Fisher Scientific, Pittsburgh, PA), stained with toluidine blue, and

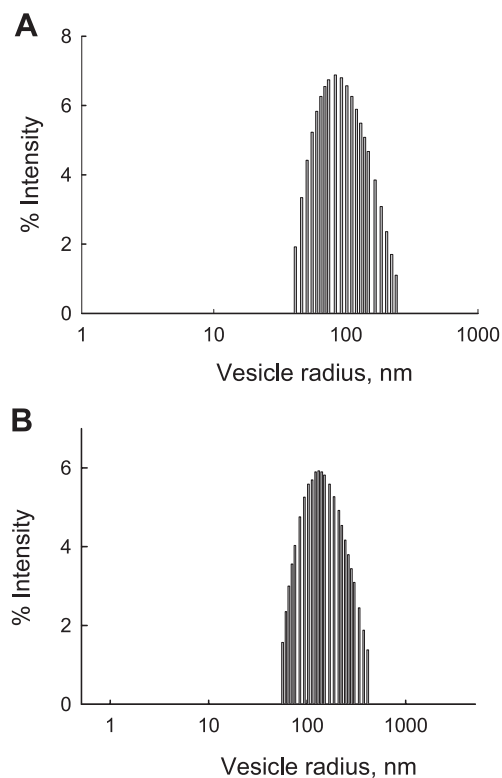


Fig. 1. Size distribution of apical and basolateral vesicles. Vesicle size was measured by laser light scatter (see MATERIALS AND METHODS). Apical (A) and basolateral membrane vesicles (B) showed a single population of vesicles with an average radius of 126 and 188 nm, respectively.

then mounted under a coverslip using Aqua Polymount mounting medium (Polysciences, Warrington, PA).

Estimation of gland volume using the Cavalieri method. Images were obtained by scanning the individual sections of each tissue block using a Nikon Coolscan III slide scanner. The images were printed at 2× magnification, a randomly translated point grid was placed on the image, and the number of points (P_i) falling on glandular tissue was quantified. The volume of each gland was estimated using the following formula (13):

$$V_{\text{gland}} = T \cdot \frac{a}{p} \cdot \sum_{i=1}^n P_i$$

In our analysis, the section thickness (T) was 0.5 mm, the area per point (a/p) was determined to be 1.96 mm², and the number of sections measured (n) varied from 7 to 9 depending on the length of the gland. The volume estimates obtained using this method were in good agreement with volumes obtained by measuring fluid displacement.

Estimation of tubule volume in rectal gland. The average volume fraction for epithelial tubules ($V_{\text{v tubule}}$) was determined by placing a randomly translated point grid on scanned images (magnified ×25) and then determining the ratio of points falling on epithelial tubules [$P_{\text{(tubule)}}$] relative to points falling anywhere on glandular tissue [$P_{\text{(gland)}}$] as described by the following formula (13):

$$V_{\text{v tubule}} = \frac{\sum_{i=1}^n P_{\text{(tubule)}}}{\sum_{i=1}^n P_{\text{(gland)}}$$

The mean tubular volume (V_{tubule}) was calculated by multiplying the volume fraction of the tubules by the volume of the gland.

Estimation of apical surface area of epithelial cells lining the tubules. The surface density of membrane lining the epithelial tubules ($S_{\text{v apical surface}}$) was determined by overlaying a cycloid lattice grid on randomly acquired images (obtained using a digital camera) printed at a final magnification of ×550. Intersections of the cycloids with the apical surface domains lining the lumen of the tubules (I) along with the number of points falling on tubules (P) were counted. The surface density ($S_{\text{v apical surface}}$) was calculated using the following formula (13):

$$S_{\text{v apical surface}} = 2(p/l) \frac{\sum_{i=1}^n I_i}{\sum_{i=1}^n P_i}$$

Where (p/l) is the ratio of test points to test curve length and is a function of the cycloid grid, which in this case was 1/0.031 mm. The estimated surface area of luminal membrane ($S_{\text{apical surface}}$) was determined by multiplying the $S_{\text{v apical surface}}$ by the volume of the cell.

RESULTS

Purity of vesicle preparations. To ensure that the vesicles represented apical and basolateral membranes, respectively, immunoblots were performed to determine whether the *S. acanthius* CFTR was expressed in the apical fraction and whether Na-K-ATPase α -subunit was expressed in the basolateral fraction. Figure 2 shows a representative set of blots. Figure 2, left, shows labeling for Na-K-ATPase was found only

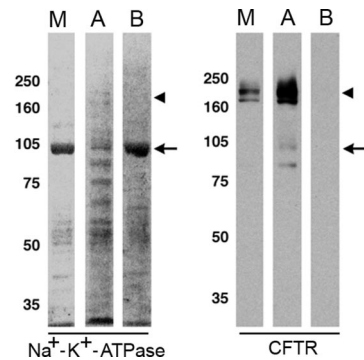


Fig. 2. Membrane vesicle enrichment and purity. Enrichment of Na⁺-K⁺-ATPase α -subunit in basolateral (B) membranes and cystic fibrosis transmembrane regulator (CFTR) in apical (A) membranes resolved by sucrose gradient centrifugation of shark rectal gland microsomes (M). *Left*: 3 lanes show the very abundant Na⁺-K⁺-ATPase α -subunit is detected by staining with Coomassie brilliant blue (band position indicated by arrow). *Right*: corresponding immunoblots in 3 lanes were probed with an antibody to shark CFTR, 60.1 (bands indicated by arrowhead).

in the microsomal fraction and the basolateral preparation. In Fig. 2, right, labeling for CFTR was found only in the microsomal fraction and the apical preparation. Note that the final preparations are being compared with the microsomal fraction, rather than the whole homogenate. There is modest purification of the Na-K-ATPase α -subunit in the purified basolateral fraction. This is likely to be the case because the markedly ramified basolateral membrane of the rectal gland epithelial cell represents a large proportion of the microsomal membranes (2, 3, 6). By contrast, the apical membrane fraction exhibits marked purification of CFTR, indicating that the sucrose gradient procedure highly purifies this membrane.

Permeabilities of basolateral membrane vesicles. Figures 3 and 4 show representative water and urea fluxes, as well as activation energies for water flux for basolateral (Fig. 3) and apical (Fig. 4) membrane fractions. For both water and urea fluxes, the curves reveal single populations of vesicles, and the data are well fit by single exponential functions, permitting calculation of permeability values. It is important to note here that the vesicles behaved as a single population in both the sizing studies and the permeability measurements. On this basis, even if there are impurities in the preparations, it is highly likely that the permeability values obtained reflect the properties of the apical and basolateral membranes of the epithelium, respectively.

At 8.8°C, water permeability across basolateral membrane vesicles averaged $4.3 \pm 1.3 \times 10^{-3}$ cm/s, while at 15°C urea permeability in the same vesicles averaged $4.2 \pm 0.8 \times 10^{-7}$ cm/s (Fig. 3). To determine whether water permeation might occur via aquaporin water channels, water flux was measured at different temperatures and the E_a for water transport was calculated; the values are plotted in Fig. 3C. E_a averaged 16.4 kcal/mol in two separate preparations, a value far above the 4–5 kcal/mol that is characteristic of flux through water channels (25).

Permeabilities of apical membrane vesicles. Figure 4 shows water and urea fluxes across apical membrane preparations. At 8.8°C, apical membrane vesicle water permeability averaged $7.5 \pm 1.6 \times 10^{-4}$ cm/s, while at 15°C urea permeability in these preparations averaged $2.2 \pm 0.4 \times 10^{-7}$ cm/s. Using a

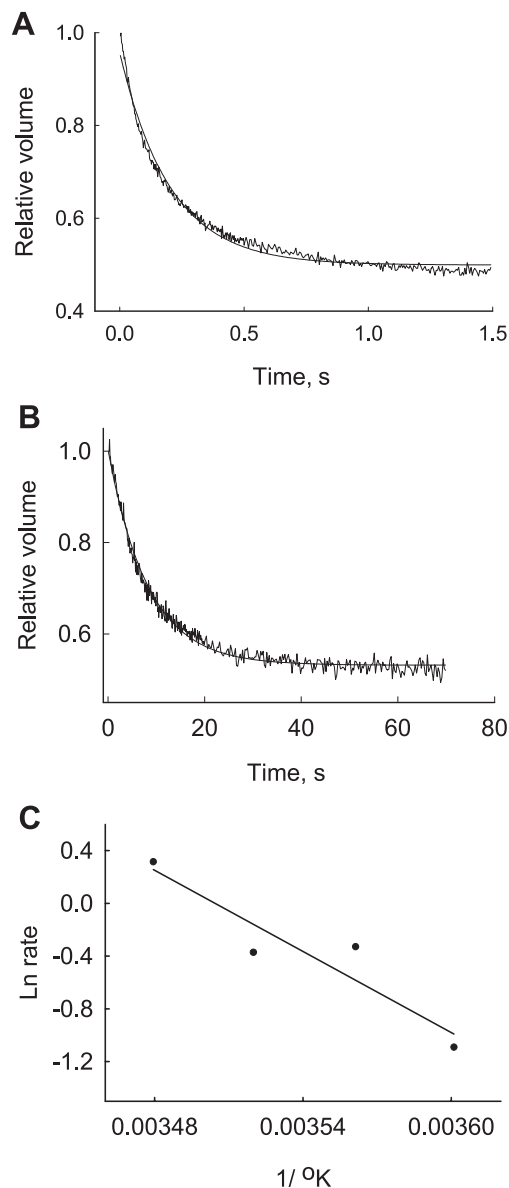


Fig. 3. Permeability of basolateral membrane vesicles. Time course of relative volume changes of water (A) and urea (B) efflux. Permeability values were computed from the single exponential fits as described in MATERIALS AND METHODS. C: temperature dependence of water permeability. The calculated value of activation energy (see MATERIALS AND METHODS) for water permeability is 16.4 kcal/mol.

standard *t*-test, the water permeability values were not statistically different between the apical and basolateral membrane preparations ($0.05 \leq P \leq 0.1$), whereas the urea permeabilities did reach statistical significance ($P \leq 0.05$). The E_a for water flux averaged 18.6 kcal/mol in two preparations, again indicating that water flux is not occurring via aquaporins (25).

Relationship between water and urea permeabilities. In prior studies using artificial liposomes, we found that water and urea permeabilities varied linearly with each other, so that artificial membranes that exhibited low water permeabilities also restricted urea flux, whereas membranes that permitted high water flux also exhibited high urea permeabilities. To determine whether this relationship holds true over a wide array of liposomes, as well as biological membranes, we

plotted in Fig. 5 water and urea permeabilities of all liposome and isolated membrane vesicle preparations that we previously published. Figure 5A shows measurements performed in liposomes, including lipids derived from *archaeobacteria*, *eubacteria*, and mammals. It is apparent that, for lipid bilayers, urea permeability is linearly related to water permeability, with an *r* value of 0.94.

To determine whether this property holds for freshly isolated membrane vesicles, we graphed all of our prior results, including apical and basolateral membranes from a wide variety of tissues, as well as permeabilities measured in Ussing chambers in intact mammalian bladders (with appropriate subtraction of unstirred layer effects). We omitted membranes that are known to contain aquaporin water channels. Because our research effort focused on membranes that act as barriers to water flow, most of the values in Fig. 5B are clustered in the lower range of water permeabilities. With these caveats, these results are

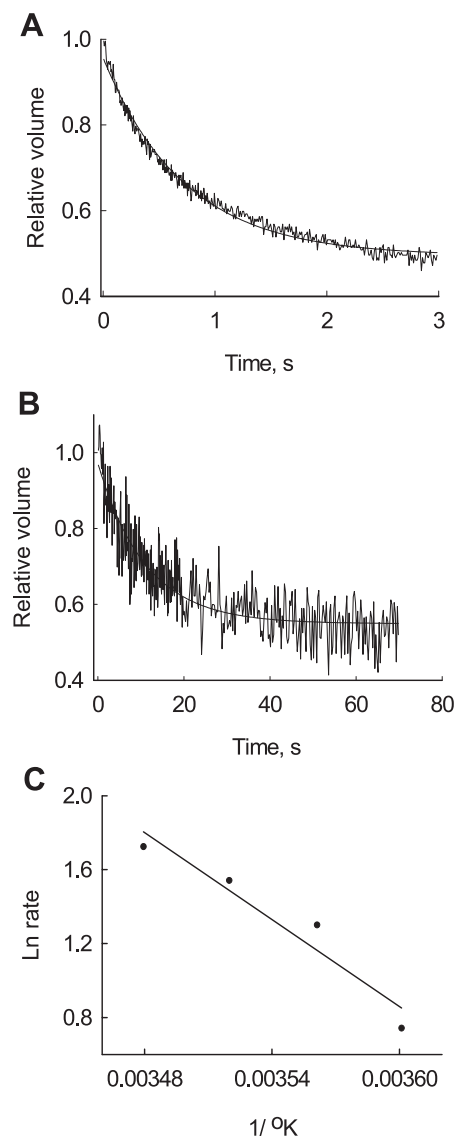


Fig. 4. Permeability of apical membrane vesicles. Tracings of relative volume changes due to water (A) and urea (B) efflux as a function of time. Permeability values were calculated as in Fig. 3. Activation energy value (C) calculated from temperature dependence of water permeability is 18.6 kcal/mol.

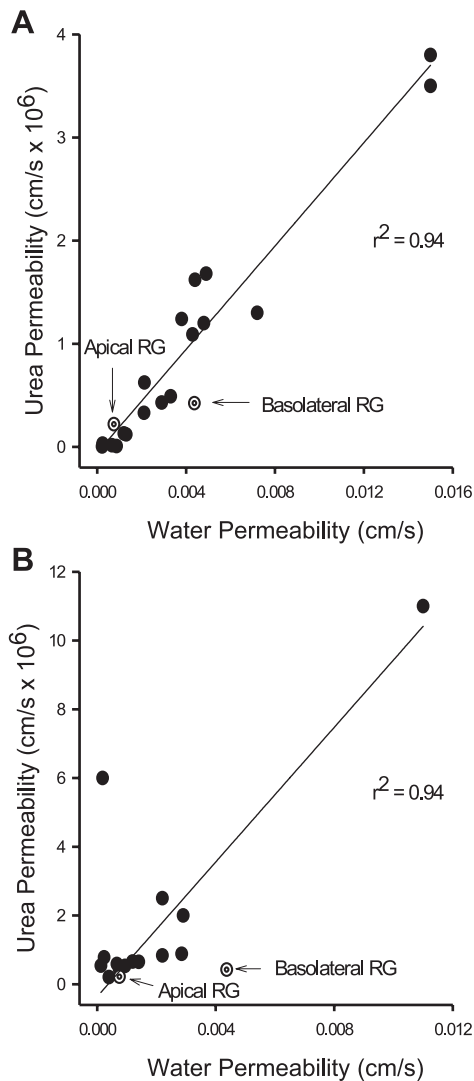


Fig. 5. Comparison of water and urea permeability. A plot of water and urea permeability in artificial (A) and native (B) membrane vesicles shows a good correlation of urea permeability with water permeability. ● Represent values from prior studies. Unfilled circles represent values from the current study. A and B: values from basolateral membrane vesicles (basolateral RG) and from apical vesicles (apical RG) are identified and labeled as well. Values from prior studies were obtained from Refs. 5, 9, 10–12, 15, 16, 18, and 20–22.

linear as well as indicating that for most biological membranes, urea permeability is directly proportional to water permeability.

On both graphs, we placed the values obtained in the current study. It is apparent that the apical membrane urea and water permeabilities fit well with the liposomal or the membrane vesicle data. By contrast, the basolateral membrane urea per-

meability is nearly 10-fold lower than expected, given the relatively high water permeability of the basolateral membrane.

Surface areas of apical and basolateral membranes. We measured the total surface areas for five rectal glands, with values ranging from 19,000 to 50,000 mm². For three of the samples, the weights of the sharks were recorded and the measurements for these three samples are shown in Table 1. From these three glands, apical membrane surface area averaged 30,000 mm²/kg shark weight.

DISCUSSION

The rectal gland of the dogfish elaborates a fluid that is isotonic with plasma but which is relatively enriched in NaCl and has a very low concentration of urea when compared with plasma values (2, 3). Because elasmobranchs must maintain high tissue and plasma urea concentrations to prevent the loss of body water to the ocean, it is important that the rectal gland secretes a fluid that is low in urea.

The rectal gland is known to secrete sodium chloride, with water following the ion fluxes passively. Because the osmolality of the elaborated rectal gland fluid equals that of the plasma, it appears likely that any osmotic gradients that drive water flux must be small and transient and are likely confined to regions close to the surface of secretory cells. On this basis, we anticipated that the water permeability of rectal gland membranes would be high, whereas urea permeability remained low. Since our prior studies (now summarized in Fig. 5) showed that high water permeabilities are accompanied in artificial liposomes and membrane vesicles by high urea permeabilities, we hypothesized that the rectal gland would have aquaporin water channels.

To test this hypothesis, we first needed to isolate both apical and basolateral membranes from rectal gland epithelia. Examination of the structure of the rectal gland reveals that basolateral membrane surface area is many fold larger than apical membrane surface area (2, 6). On this basis, the initial microsomal membrane fraction would be expected to contain a great deal of basolateral membrane and a small amount of apical membrane. Therefore, the modest purification of Na-K-ATPase α -subunit observed in the basolateral fraction can be explained by relatively high levels in the fraction with which it is being compared, the microsomal fraction. In other words, the basolateral membrane is already purified to a great degree in the microsomal fraction. The fact that the ATPase is markedly depurified in the apical fraction and that CFTR is markedly purified in this fraction provides strong evidence that this fraction represents highly purified apical membranes. The differing sizes and permeability properties of the preparations indicate that they are distinct vesicle populations. In addition, the fact that each fraction behaves as a single population on

Table 1. Summary of data for rectal glands

Gland and Shark Weight	Volume of Gland, mm ³	V _{v tubule}	V _{tubule} , mm ³	S _{v apical surface} , mm ⁻¹	S _{apical surface} , mm ²	S _{apical surface/kg body wt} , mm ²
1.5 kg	1,509.2	0.378	584.1	57.26	33,554.6	22,297.0
0.5 kg	980	0.279	273.4	75.00	20,506.5	41,013.0
0.75 kg	1,234.0	0.296	365.3	72.18	26,367.4	35,156.5

V_{v tubule}, fraction of total volume that is tubules; V_{tubule}, total volume of tubules in gland; S_{v apical surface}, amount of apical membrane surface area per unit volume of tubule; S_{apical surface}, total surface area of apical membrane in gland.

permeability and sizing studies indicates that the permeabilities measured reflect those of the membrane in question, even if the fractions have some impurities in them. In prior studies we noted that vesicle preparations containing more than one type of vesicle exhibit bimodal size distributions and exhibit complex exponential (i.e., not single exponential) flux curves (10). Indeed, we have been able to detect different permeabilities in fractions as small as 10% of the whole fraction of vesicles (Mathai JC, Hill W, and Zeidel ML, unpublished observations).

Because the basolateral membrane exhibits higher permeabilities to water and urea than the apical membrane, and because the basolateral membrane has a vastly greater surface area than the apical membrane, it is clear that the apical membrane represents the rate-limiting membrane for both water and urea flux across the rectal gland epithelium.

The measured apical membrane water permeability is relatively low for a membrane that may contain a water channel. Generally, water channel-containing membranes exhibit water permeabilities in the range of 10^{-2} cm/s. In addition, the high E_a for water flow indicates that water is crossing through the lipid portion of the membrane, rather than via a protein channel. Although the water permeability of the basolateral membrane is higher than that of the apical membrane, the high E_a again makes it unlikely that an aquaporin mediates the water flow across this membrane. Because the rectal glands used to prepare the membranes were not stimulated with exogenous agents to secrete salt before death, it is still possible that under hormonal stimulation a water channel might be inserted into the apical or basolateral membranes. It is likely, however, that several of the sharks were actively excreting salt when they were killed for these preparations. Moreover, the presence of dogfish CFTR in the apical membrane fractions (see Fig. 2) suggests that much of the membrane was taken from glands that were capable of actively secreting chloride just before death.

To determine whether the permeabilities measured in these preparations can account for the behavior of the rectal gland *in vivo*, we estimated the amount of urea loss expected to occur in a day across the rectal gland. Because the apical membrane has a smaller surface area and lower urea permeability than the basolateral membrane, we considered the apical membrane to be the rate-limiting barrier to urea loss.

To determine the expected urea permeation across the rectal gland, we used the standard permeability equation:

$$\text{Flux}_{\text{urea}} = (P_{\text{urea}}) \times (\text{SA}) \times (\Delta\text{Urea})$$

Where ΔUrea is the urea concentration gradient (330–18 mM), and surface area is 30,000 mm². We are assuming in this calculation that the concentration of urea within the rectal gland epithelial cell is the same as that of the plasma. Using these values, we anticipate that the shark will lose 1.8 mmol of urea per day. Because the plasma concentration is 330 mmol/l, and water constitutes 70% of the shark's weight, the total urea content of a 1-kg shark is 231 mmol (1–3, 8). On this basis, the shark would be expected to lose only 0.8% of its urea content in a day. Of course, the animal actually loses 0.22 mmol of urea/day (18 mmol/l of rectal gland fluid \times 0.5 cm³/h of secretion) (1–3, 8).

Alternatively, there may be additional barriers to urea flux in the rectal gland. For example, it is possible that the concentration of urea within the cell is lower than that in the plasma. The basolateral membrane exhibits a strikingly low urea permeability (especially in view of its water permeability), although its relatively large surface area may permit relatively rapid movement of urea into the cell. A urea gradient between the plasma and the interior of the cell could persist across this membrane only if there is some sort of urea transport activity, which transports urea back out to the basolateral side. Indeed, Northern blot analysis of dogfish shark rectal gland showed the presence of urea transporter, ShUT; however, its protein localization and its actual function in the tissue are not clear (24). Although there is no evidence that shUT can transport urea "uphill" against a concentration gradient, it is possible that an active transporter pumps urea up its chemical gradient from inside the epithelial cell across the basolateral membrane back into the blood. Such active transport of urea could be effected by a carrier-mediated mechanism, with urea coupled to the transport of another substance down its electrochemical gradient. Saturable carrier-mediated transport of urea has been demonstrated in the gill of the trout (19). In addition, a gill elasmobranch transporter that couples urea transport to that of sodium has recently been identified (7). This latter mechanism would reduce the concentration of urea within the cell and lead to lower flux of urea into the rectal gland fluid than would be predicted by our permeability measurements.

Fines et al. (7) found that gill membrane vesicles contained extremely high ratios of cholesterol to phospholipids and suggested that this membrane composition could form a barrier to urea. A similar lipid composition in the rectal gland membranes might reduce urea permeation. However, as shown in Fig. 5, the basolateral urea permeability is much lower than would be expected, considering its water permeability. In other words, a lipid composition capable of severely limiting urea flux should also severely limit water flux. In the absence of an aquaporin, how is this low urea permeability achieved in the face of a relatively high water permeability? As prior studies in liposomes of widely varying lipid structure (Fig. 5) have never identified a selectivity barrier for urea, as opposed to water, it appears likely that the selectivity barrier in the basolateral membrane is not due to unique lipid structure. Alternatively, it is possible that a protein component of this membrane renders it selectively impermeable to urea, in much the same way that certain claudins prevent water from crossing the tight junctions of medullary thick ascending limbs while allowing cations to pass (23).

ACKNOWLEDGMENTS

We thank J. Forrest for assistance in obtaining rectal glands for morphometric analysis and F. Epstein, D. Evans, and R. Kinne for helpful comments.

REFERENCES

1. **Boylan JW.** Gill permeability in *Squalus acanthias*. In: *Sharks, Skates and Rays*, edited by Gilbert PW, Mathewson RF, and Rall DP. Baltimore, MD: Johns Hopkins Press, 1967.
2. **Burger JW.** Problems in the electrolyte economy of the spiny dogfish, *Squalus acanthias*. In: *Sharks, Skates and Rays*, edited by Gilbert PW, Mathewson RF, and Rall DP. Baltimore, MD: Johns Hopkins Press, 1967.
3. **Burger JW and Hess WN.** Function of the rectal gland in the spiny dogfish. *Science* 131: 670–671, 1960.

4. **Carrier JC and Evans DH.** Ion, water and urea turnover rates in the nurse shark, *Ginglymostoma cirratum*. *Comp Biochem Physiol A* 41: 761–764, 1972.
5. **Chang A, Hammond TG, Sun TT, and Zeidel ML.** Permeability properties of the mammalian bladder apical membrane. *Am J Physiol Cell Physiol* 267: C1483–C1492, 1994.
6. **Dubinsky WP and Monti LB.** Resolution of apical from basolateral membrane of shark rectal gland. *Am J Physiol Cell Physiol* 251: C721–C726, 1986.
7. **Fines GA, Ballantyne JS, and Wright PA.** Active urea transport and an unusual basolateral membrane composition in the gills of a marine elasmobranch. *Am J Physiol Regul Integr Comp Physiol* 280: R16–R24, 2001.
8. **Goldstein L.** Urea biosynthesis in elasmobranchs. In: *Sharks, Skates and Rays*, edited by Gilbert PW, Mathewson RF, and Rall DP. Baltimore, MD: Johns Hopkins Press, 1967.
9. **Grossman EB, Harris HW, Star RA, and Zeidel ML.** Water and nonelectrolyte permeabilities of highly purified apical membranes of toad urinary bladder granular cells. *Am J Physiol Cell Physiol* 262: C1109–C1118, 1992.
10. **Hill WG, Mathai JC, Gensure RH, Zeidel JD, Apodaca G, Saenz JP, Kinne-Saffran E, Kinne R, and Zeidel ML.** Permeabilities of teleost and elasmobranch gill apical membranes: evidence that lipid bilayers alone do not account for barrier function. *Am J Physiol Cell Physiol* 287: C235–C242, 2004.
11. **Hill WG, Rivers RL, and Zeidel ML.** Role of leaflet asymmetry in the permeability of model biological membranes to protons, solutes, and gases. *J Gen Physiol* 114: 404–414, 1999.
12. **Hill WG and Zeidel ML.** Reconstituting the barrier properties of a water-tight epithelial membrane by design of leaflet-specific liposomes. *J Biol Chem* 275: 30176–30185, 2000.
13. **Howard CV and Reed MG.** *Unbiased Stereology. Three Dimensional Measurement in Microscopy*. New York: Springer-Verlag, 1998.
14. **Karnaky K.** *Osmotic and Ionic Regulation*. New York: CRC, 1997.
15. **Lande MB, Donovan JM, and Zeidel ML.** The relationship between membrane fluidity and permeabilities to water, solutes, ammonia, and protons. *J Gen Physiol* 106: 67–84, 1995.
16. **Lande MB, Priver NA, and Zeidel ML.** Determinants of apical membrane permeabilities of barrier epithelia. *Am J Physiol Cell Physiol* 267: C367–C374, 1994.
17. **Loo MA, Jensen TJ, Cui L, Hou YX, Chang XB, and Riordan JR.** Perturbation of Hsp90 interaction with nascent CFTR prevents its maturation and accelerates its degradation by the proteasome. *EMBO J* 17: 6879–6887, 1998.
18. **Mathai JC, Sprott GD, and Zeidel ML.** Molecular mechanisms of water and solute transport across archaeobacterial lipid membranes. *J Biol Chem* 276: 27266–27271, 2001.
19. **McDonald MD and Wood CM.** Evidence for facilitated diffusion of urea across the gill basolateral membrane of the rainbow trout (*Oncorhynchus mykiss*). *Biochim Biophys Acta* 1663: 89–96, 2004.
20. **Piqueras AI, Somers M, Hammond TG, Strange K, Harris HW Jr, Gawryl M, and Zeidel ML.** Permeability properties of rat renal lysosomes. *Am J Physiol Cell Physiol* 266: C121–C133, 1994.
21. **Priver N, Rabon E, and Zeidel ML.** The apical membrane of the gastric parietal cell: water, proton, and nonelectrolyte permeabilities. *Biochemistry* 32: 2459–2468, 1993.
22. **Rivers R, Blanchard A, Eladari D, Leviel F, Paillard M, Podevin RA, and Zeidel ML.** Water and solute permeabilities of medullary thick ascending limb apical and basolateral membranes. *Am J Physiol Renal Physiol* 274: F453–F462, 1998.
23. **Simon DB, Lu Y, Choate KA, Velazquez H, Al-Sabban E, Praga M, Casari G, Bettinelli A, Colussi G, Rodriguez-Soriano J, McCredie D, Milford D, Sanjad S, and Lifton RP.** Paracellin-1, a renal tight junction protein required for paracellular Mg^{2+} resorption. *Science* 285: 62–64, 1999.
24. **Smith CP and Wright PA.** Molecular characterization of an elasmobranch urea transporter. *Am J Physiol Regul Integr Comp Physiol* 276: R622–R626, 1999.
25. **Zeidel ML, Ambudkar SV, Smith BL, and Agre P.** Reconstitution of functional water channels in liposomes containing purified red cell CHIP28 protein. *Biochemistry* 31: 7436–7440, 1992.

